Sodium Magnetic Resonance Imaging of Chemotherapeutic Response in a Rat Glioma

Victor D. Schepkin,* Brian D. Ross, Thomas L. Chenevert, Alnawaz Rehemtulla, Surabhi Sharma, Mahesh Kumar, and Jadranka Stojanovska

This study investigates the comparative changes in the sodium MRI signal and proton diffusion following treatment using a 9L rat glioma model to develop markers of earliest response to cancer therapy. Sodium MRI and proton diffusion mapping were performed on untreated (n = 5) and chemotherapy 1,3-bis(2-chloroethyl)-1-nitrosourea-treated rats (n = 5). Animals were scanned serially at 2- to 3-day intervals for up to 30 days following therapy. The time course of Na concentration in a tumor showed a dramatic increase in the treated brain tumor compared to the untreated tumor, which correlates in time with an increase in tumor water diffusion. The largest posttreatment increase in sodium signal occurred 7–9 days following treatment and correlated to the period of the greatest chemotherapy-induced cellular necrosis based on diffusion and histopathology. Both Na MRI and proton ADC mapping revealed early changes in tumor sodium content and cellularity. This study demonstrates the possibility of Na MRI to function as a biomarker for monitoring early tumor treatment and validates the use of monitoring changes in diffusion MRI values for assessing tumor cellularity. Magn Reson Med 53:85–92, 2005. © 2004 Wiley-Liss, Inc.

Key words: sodium; MRI; chemotherapy; diffusion; glioma

Sodium MRI is becoming increasingly attractive as a potential marker of anticancer therapeutic response by virtue of characterization of cellular properties distinct from those represented on proton MRI. Sodium investigations also benefit from a better understanding of tumor microenvironment (1–5) and advances in MRI technique and high magnetic field technology, which allow application to humans (6–15).

In our study we investigated the sequence of changes in the Na MRI signal in a brain tumor model following application of a therapeutic agent, with the objective of evaluating sodium MRI as biomarker of tumor treatment response. Moreover, diffusion mapping was also performed since it has been shown that an increase in water diffusion values occurs early following treatment due to loss of cell membrane integrity and decreased cellularity prior to tumor shrinkage (16,17). The underlying hypothesis of the detected increase in diffusion is based on therapy-induced cell destruction leading to a relative increase in water mobility. Given the normal trans-membrane cellular sodium gradient it would be expected that the tumor sodium signal would also exhibit a temporal change following effective therapy.

Intracellular Na concentration is ~15 mM, while extracellular Na concentration is ~140 mM. Consequently, during complete cell destruction a large increase in Na tumor content may take place. Based on the above values along with the fact that the extracellular space is ~0.15 of the total water space in brain, there can be theoretically an increase in Na level up to 4 times. An increase of up to approximately 1.5 times relative to normal brain was detected in study of human brain tumors (14). An increase of up to 1.8 times relative to pretreatment Na concentration was found in a radiation-treated C6 rat glioma model (18). Elevation of tumor Na concentration and ADC increase during treatment may be related, but at the same time sodium may yield more functional cellular information (19–22) as sodium tissue concentration may experience changes during interventions without any cellular membrane destruction. Thus, the ultimate goal of the present study was to investigate the relationship between the evolution in tumor sodium and tumor water diffusion using the 9L rat brain tumor model in response to the chemotherapeutic agent 1,3 bis(2-chloroethyl)-1-nitrosurea (BCNU).

METHODS

Cell Culture

Rat 9L gliosarcoma cells (Brain Tumor Research Center, UCSF) were maintained and grown as monolayer cultures in Dulbecco's modified Eagle's medium (DMEM) supplemented with 10% (v/v) heat-inactivated fetal bovine serum, 100 IU/mL penicillin, and 100 μg/mL streptomycin at 37°C in a normally humidified atmosphere containing 95% air/5% CO_2. Prior to implantation, cells were grown to confluence in a 175-cm^2 flask and harvested using a 0.25% trypsin/0.1% EDTA solution and counted. Cells were pelleted (800 × g, 5 min) and resuspended in serum-free DMEM at a concentration of ~10^5 cells/10 μL and kept on ice until use. Cell culture reagents were obtained from Invitrogen Life Technologies (Carlsbad, CA).

Tumor Implantation of Animals

Male Fisher 344 rats were obtained at 6–7 weeks of age (116–135 g) from Harlan (Indianapolis, IN). Animals (n = 10) were anesthetized by intraperitoneal injection using an 87%/13% (v/v) ketamine/xylazine mixture and then secured in a stereotactic head frame. In aseptic conditions, using a No. 10 scalpel, an incision (~2 cm) was made to

Department of Radiology, Center for Molecular Imaging, University of Michigan Medical School, Ann Arbor, Michigan.

Grant sponsor: John and Suzanne Munn Endowment Research Grant; Grant sponsor: Michigan Comprehensive Cancer Center; Grant sponsor: NIH; Grant numbers: P01 CA85878–01A2, 5 R24 CA83099–03, 1P50 CA93990–01.

*Correspondence to: Victor Schepkin, Center for Molecular Imaging, Department of Radiology, University of Michigan Medical School, Kresge II Research Building, R3028, 200 Zina Pitcher Place, Ann Arbor, MI 48109-0503. E-mail: vschepki@umich.edu

Received 29 June 2004; revised 23 August 2004; accepted 26 August 2004.
DOI 10.1002/mrm.20332
Published online in Wiley InterScience (www.interscience.wiley.com).

expose the skull and a 0.9-mm-diameter burr hole was drilled over the right forebrain using a high-speed drill (FST, Foster City, CA). For each animal, 10 μL of 9L cells (~10^5 cells) were injected at a depth of 2.5 mm. The surgical field was then cleansed using 70% ethanol and the burr hole was filled with bone wax to minimize extracerebral growth of the tumor.

Chemotherapeutic Treatment

Seventeen days after the tumor implantation, 10 tumor-bearing rats were divided into two groups of 5 (treated and control). The treated group received BCNU therapy. The average size of the tumor at the moment of treatment was ~50 μL. Standard 100 mg BCNU preparation (Bristol Lab) was dissolved in 3 mL of ethanol. Part of this solution (0.3 mL) was dissolved in 2.7 mL of saline and immediately used for IP injection (~1.3 mL). The BCNU dose of injection was 26.6 mg/kg, which is equivalent to double an LD_{10} dose. All animal experiments were conducted according to the protocols approved by the University of Michigan Committee on Use and Care of Animals.

Three additional normal rats served as a second control to evaluate possible changes in brain Na concentration during animal aging and stability of Na MR signals during the 50-day interval of these experiments.

MR Imaging

Sodium and proton MRI were performed periodically on all animals to follow the full course of tumor growth beyond date of treatment until sacrifice. Proton and sodium MR scans have been performed on two different scanners and the animals had to be repositioned between proton and sodium acquisitions. One system (9.4-T Varian MR scanner, 120-mm clear horizontal bore) was configured for all sodium scans, and an adjacent system (7-T Varian MR scanner, 110-mm clear horizontal bore) was used for all proton MRI. For every given tumor-bearing animal and a time point, the interval between sodium and proton acquisitions was approximately 1 hr, and each animal was scanned every 2 to 3 days. The same imaging protocol was used for normal rats without tumor ($n = 3$), but these were scanned only once per week over a 50-day period. With the purpose of helping the animals to support their body temperature during MRI scan all animals were placed on a temperature-controlled circulating-water heating pad. Anesthesia was achieved by breathing of 1% v/v isoflurane/air gas mixture.

Sodium MRI

The tumor region of the rat brain was placed near the center of the homebuilt Na RF coil having an internal diameter of 32 mm and length of 45 mm. Rat heads were positioned in the RF coil to within ±1 mm using the eyes as reference points. The axial length of the RF homogenous region (~6%) was approximately 14 mm, which was sufficient to encompass the spatial extent of the tumors and allow quantitative tumor sodium imaging. Because sodium has short T_2 relaxation time components, a 3D back-projection pulse sequence was used. The concept of the back-projection MR imaging was first suggested by Lauterbur in 1973 (23). The original spin-echo 3D back-projection pulse sequence (Varian, Inc.) included two hard pulses and provided an echo time of 500 μsec. The other parameters were: readout gradient 1.3 G/cm, FOV 64 × 64 × 64 mm, acquisition matrix 32 × 32 × 32, TR = 0.1 sec, and scan time = 30 min. Duration of the 90° pulse was 50 μsec. Sodium T_1 relaxation time in normal rat brain in our experiments was 38.1 ± 1.5 msec at 9.4 T, thus yielding almost unsaturated Na signal during 3D imaging. Back-projection reconstruction was performed using vendor-provided software with zero-filling to give a matrix of 128 × 128 × 128 voxels for the sodium signal through the rat brain.

Proton MRI

Protocol for proton MRI included proton T_2-weighted FSE and diffusion weighted multislice scans with total scan time of 26 min. Parameters for FSE scan were: FOV 30 × 30 mm, matrix 128 × 128, 13 slices, slice thickness 1 mm, interslice distance 1.5 mm, TR = 6 sec, TE_{eff} = 60 msec, and echo train length = 8. Parameters for the diffusion scan were: FOV 30 × 30 mm, matrix 128 × 128, 13 slices, slice thickness = 1 mm, interslice distance = 1.5 mm, spin echo with TR = 3 sec, and TE = 60 msec. The diffusion sequence employed isotropic diffusion weighting by orthogonalization of *x*-, *y*-, and *z*-gradient waveforms. That is, imaging plus diffusion gradient waveforms were designed to equalize diagonal elements and zero out off-diagonal elements of the *b*-matrix. In addition, this sequence included first-order motion compensation and a 32-point navigator echo for phase-correction prior to 2DFT image reconstruction. Diffusion weighted images (DWI) at two-*b*-factor settings were acquired for calculation of an ADC map: "high-*b*" ($b = 1082$ sec/mm^2) and "low-*b*" ($b = 117$ sec/mm^2). Proton images and ADC maps were reconstructed in Matlab and the tumor volume and tumor average ADC were determined over a 3D VOI for each temporal measurement.

Quantification and Analysis

Three-dimensional sodium and multislice proton (FSE T_2-weighted, DWI, and ADC) were coregistered in three dimensions, wherein the "deviant" sodium MRI image set undergoes rotate-translate transform onto the "target" proton image set. In our experiments, the proton T_2-weighted MRI was used as the main registration target. This process puts all images into a common geometrical frame such that tumor VOI definition is performed on available higher quality images yet is directly applicable to quantitative images of interest (i.e., sodium and ADC).

The quantification of Na MRI data was performed as follows. Na MRI measurement of the normal rat brain (three rats, eight MRI sessions) gave the amplitude averaged over 24 measurements. This average amplitude was assigned to 45 mM, as this value for normal rat brain was already found and published by others (18,24).

Then, the values of the tumor Na signal obtained at the time point "0" (i.e., immediately before BCNU injection or 17 days after tumor implantation) from all 10 tumor-bearing animals were also averaged. This average amplitude

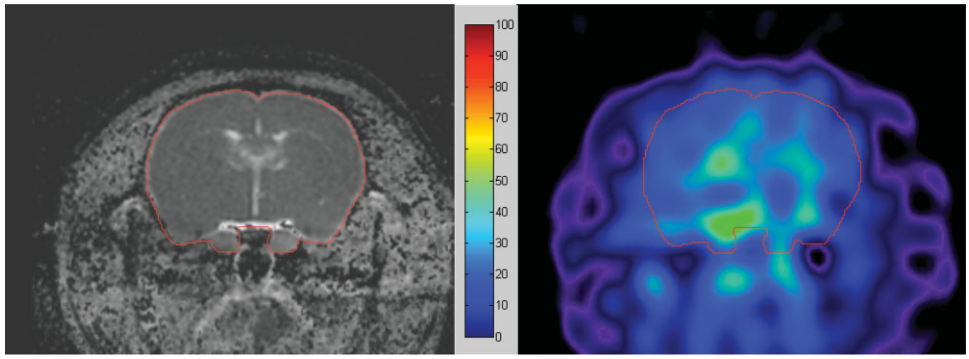

FIG. 1. Sodium MRI (right) and proton ADC map (left) MR for the matching slice position in a normal rat brain. Color bar gives the intensity scale, which is held constant for all sodium images to visually demonstrate absolute alterations in brain Na concentrations with time following therapy.

was compared with the average amplitude from the normal rats and the comparison gave us the initial tumor Na concentration at day 0 of 60 mM. This average tumor signal and the first measurements for each animal at day 0 were used to obtain the normalizing factor for this animal at zero and other time points. This step was introduced to partially offset any possible variation in intensity ~10% due to deviations in the tumor positions of individual animals inside the RF coil. Thereafter, all tumor Na signals were compared with Na signals from a normal rat brain to obtain tumor Na concentration values in millimoles.

Reproducibility of the experimental conditions for sodium imaging was periodically checked using three nontumored rats and will be demonstrated later in the paper. Sodium concentration was presented as the average ± SEM.

RESULTS

Normal Rat Brain

The typical sodium and proton images for the matching slice position in a normal rat brain are presented in Fig. 1. The sodium image clearly depicts the rat head and brain. The outline of the brain from the proton image is scribed in red and overlaid on the sodium image. The color bar for the sodium images was selected from the maximum observed tumor Na signals, which gave for the normal rat brain Na intensity around 45%. This color scale is held constant for all subsequent Na images to visually demonstrate absolute change in brain Na concentration over time following therapy.

The sodium signal intensities in normal rat brain integrated over the region corresponding to tumor in tumor-bearing animals show a reproducibility of sodium measurements in our system. These sodium signals averaged from three normal animals studied over 50 days of our experiments are plotted in Fig. 2. The Na MRI signals from the normal rat brain were extremely reproducible and remained unchanged throughout all days of the experiments. The SD of sodium MRI measurements in normal rat brain was ±4%.

Untreated Brain Tumor

Examples of images from untreated tumor-bearing animals are presented in Fig. 3. The upper row depicts Na images; below are corresponding proton ADC maps. Images in Fig. 3 were acquired at 0, 4, and 7 days. Day 0 corresponds to day 17 after 9L tumor cell implantation. The contour lines on sodium images show the position of the tumor determined from proton MR images. Tumor sodium intensities on the images are increasing in time and are distinctive from the normal brain. As can be seen in Fig. 3 the Na signals are heterogeneous throughout the tumor. On day 7, the untreated animals were sacrificed due to the large tumor size. Even at this time, the distribution of the Na signals remained heterogeneous. It is important to notice that at the rim of tumor a Na concentration was usually the lowest, while areas of high concentration of Na may reflect the location of areas with high intracellular Na concentration and/or regional necrosis. The untreated group of rats had an average survival time of 7 days (or 24 days from 9L cell implantation).

BCNU-Treated Brain Tumor

The effects of BCNU treatment on the tumor are demonstrated in Fig. 4. As for the untreated rats, a heterogeneous Na concentration can be seen throughout the tumor on the start day (day 0). The middle images were taken at day 7 following BCNU treatment. At this time an intense in-

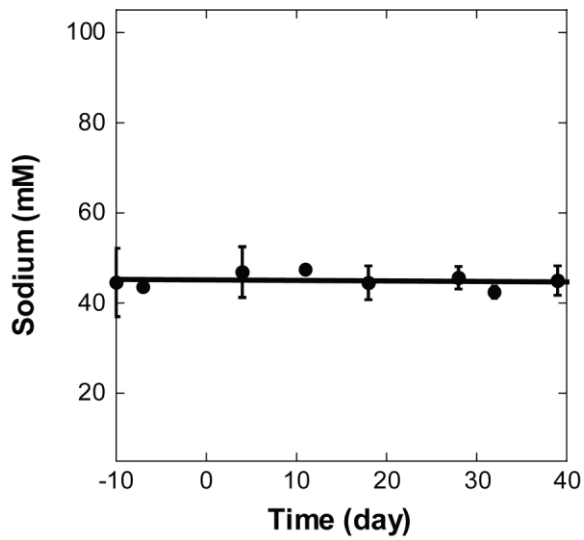

FIG. 2. Sodium MRI concentration in the normal rat brain. There was no significant trend detected over the 50-day monitoring period (n = 3). Day 0 corresponds to the time of BCNU injection in the treated group.

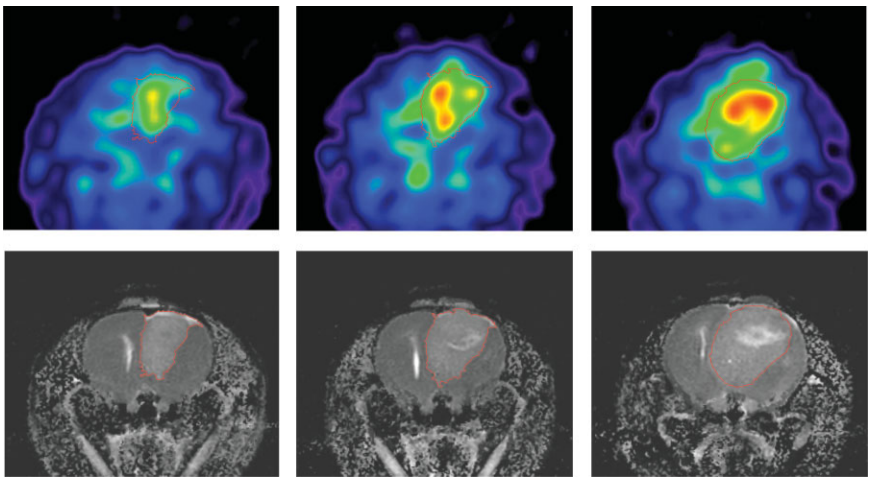

FIG. 3. Untreated 9L rat brain glioma. Sodium MRI (top) and proton ADC map (bottom) images acquired at days 0, 4, and 7 (left to right). Day 0 corresponds to the 17th day from tumor implantation. Sodium images illustrate a common feature for all untreated animals: heterogeneity in tumor Na concentration and increase of tumor Na concentration with time.

crease in Na concentration in all areas of the tumor was observed, including the rim of the tumor, and the corresponding largest increase in ADC of water in the tumor was detected. During tumor regrowth, sodium concentrations were reduced and heterogeneity in tumor Na reappeared, as shown in images acquired on day 23. Average survival time of the treated group was 28 days (or 45 days from tumor implantation).

ADC Map

Example of ADC maps showing changes of in tumor diffusion values are shown in the bottom row of Figs. 3 and 4. The matching slice positions illustrate a good correspondence in features between ADC map and sodium images. ADC maps reveal the location of necrosis within the tumor. These areas also correlate with the areas of increased Na concentration on corresponding Na images.

Increased ADC values and much more homogeneity inside the tumor were observed in treated animals, which have a strong correspondence to the areas of intense Na concentration on sodium images.

Tumor Sodium Concentration

The time course of the average sodium concentration in BCNU-treated and untreated brain tumors are given in Fig. 5. Zero time corresponds to the time immediately prior to BCNU treatment. The tumor sodium concentration in untreated rats rose steadily with a rate of ~1.6 mM/day. At the day of sacrifice the maximum tumor Na concentration was ~79 mM or 1.8 times more than in a normal rat brain.

However, the rate of sodium increase in BCNU-treated animals was 2.9 times greater (~4.7 mM/day). By day 4, the average Na concentrations in the treated animal group were statistically higher than in the untreated group. Tumor sodium reached its maximum of 100 mM, which was 2.2 times more than in a normal brain, at day 7 after treatment. The subsequent decrease in average Na concentration was correlated with tumor shrinkage. During tumor regrowth, the values of Na signals were comparable to that in tumors of untreated animals.

ADC and Tumor Volume

The time course of ADC and tumor volume in BCNU-treated 9L rat brain tumors is illustrated in Fig. 6. A well-distinguished increase in ADC indicates a positive therapeutic response. At day 4 after treatment, ADC values were statistically significant from the untreated group and reached maximum change at day 9, with subsequent tumor shrinkage occurring at day 11. During tumor regrowth,

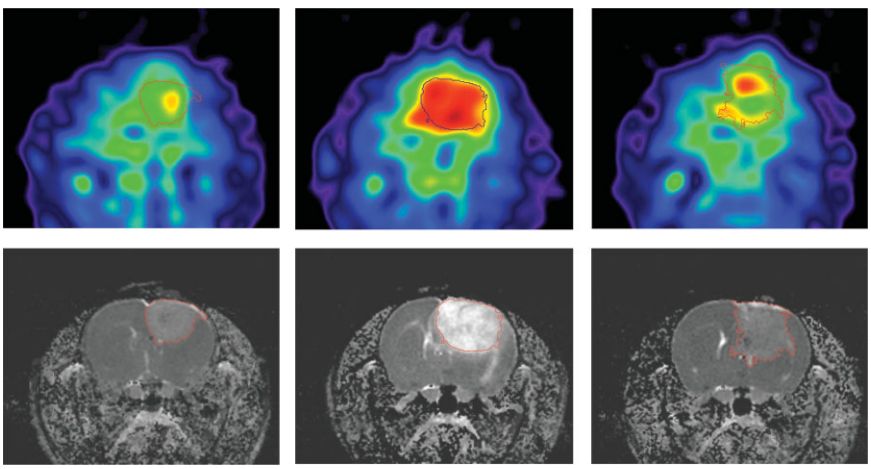

FIG. 4. BCNU-treated 9L rat glioma. Sodium MRI (top) and proton ADC maps (bottom) acquired at day 0, 7, and 23 (left to right) after BCNU injection, performed at the 17th day from tumor implantation. Central Na image at day 7 illustrates the main feature for all treated animals: a dramatic Na concentration increase observed throughout the entire tumor area. The images at day 23 show tumor during regrowth after tumor shrinking started at day 9 and its maximum regression at day 16.

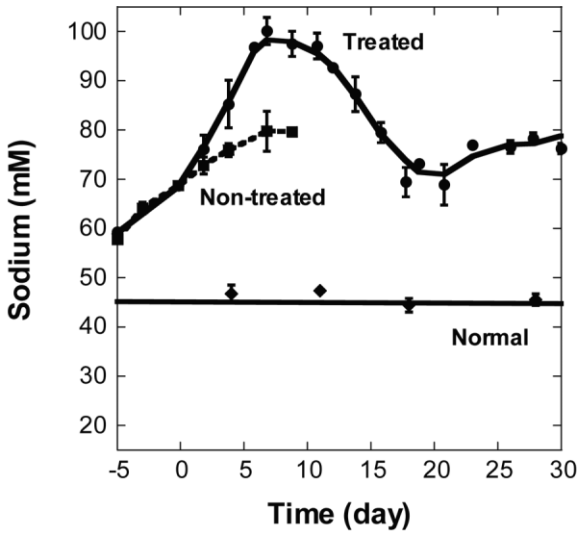

FIG. 5. Time course of tumor sodium concentration in BCNU-treated (●, $n = 5$) and untreated (■, $n = 5$) 9L rat gliomas. Time 0 corresponds to the day of BCNU treatment (17 days after tumor implantation). Accelerated rate of Na concentration increase (by 2.9 times) was observed after BCNU treatment in comparison to untreated tumors. At the bottom of the graph is the sodium concentration measured in the brain of a normal rat (♦, $n = 3$).

ADC values decreased and became comparable with the values for untreated (or pretreated) tumor.

The brain water ADC values of normal animals were measured weekly as shown at the bottom of Fig. 6. The average value of ADC in normal rats was $(0.78 \pm 0.01) \times 10^{-3}$ mm^2/sec.

The time course for ADC, sodium concentration, and tumor volumes in untreated animals is given in Fig. 7. No significant changes in ADC were detected during all the time of measurements in an untreated tumor while the tumor was constantly growing. During the same time, a steady increase in average Na tumor concentration was observed as shown in Na images (Fig. 3).

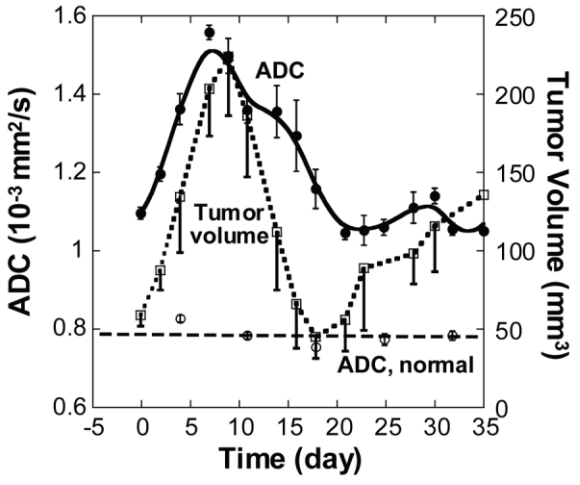

FIG. 6. Time course of water ADC in tumor (●, $n = 5$) and tumor volume (□, $n = 5$) in BCNU-treated rat gliomas. The graph at the bottom shows ADC measurement of normal rat brain (○, $n = 3$). Values of ADC during tumor growth and regrowth remain significantly above the values for normal brain. Day 0 represents the time of BCNU injection.

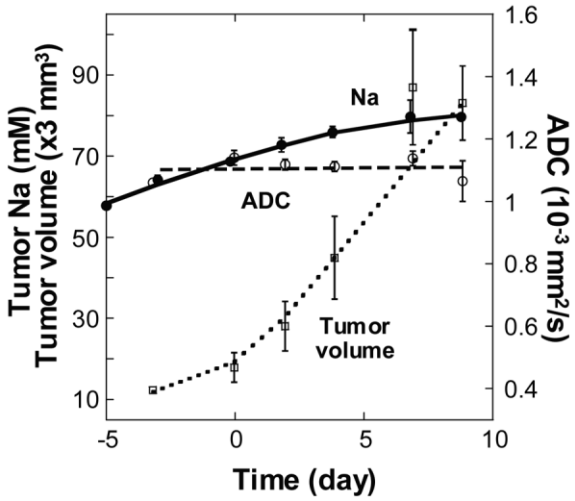

FIG. 7. Comparison of the time course for tumor Na concentration, ADC of water in the tumor, and tumor volume in untreated rat glioma model ($n = 5$). Day 0 corresponds to the 17th day from tumor implantation.

DISCUSSION

The objective of this work was to evaluate sodium MRI as a noninvasive marker of tumor response to anti-cancer therapy, as well as to correlate changes in sodium with water diffusion since the use of ADC maps has been studied extensively in preclinical studies (16,17,25). To address these objectives, the natural evolution of sodium signals in the brain of untreated tumor-bearing animals was determined and compared to that of treated animals. The rationale for investigating sodium changes relates to the sodium concentration gradient, which exists between intra- and extracellular environments. This concentration gradient consists of an approximately 10-fold sodium concentration difference in the extracellular space relative to the intracellular space. Disruption of membrane and consequently the change of trans-membrane Na gradient by way of therapies should be observed as an increase in sodium signal as a relative shift occurs to a greater volume with a higher Na concentration. An analogous principle is the basis for use of water diffusion as a therapy response indicator, when changes in tumor cellularity increase diffusion. Here, however, the probe is water mobility, which is greater in the extracellular domain.

Sodium images of the untreated rat brain tumor had demonstrable heterogeneity. The areas with the largest Na intensity have a well-defined correspondence to the high values of ADC in proton images. Within 2 to 5 days following BCNU treatment, increases in tumor Na concentration were observed. If we compare sodium images for untreated and treated animals (Figs. 3 and 4) the Na signal throughout the treated tumor mass increased and became more uniform relative to the untreated tumor. Moreover, the changes in tumor Na occurred prior to tumor shrink-

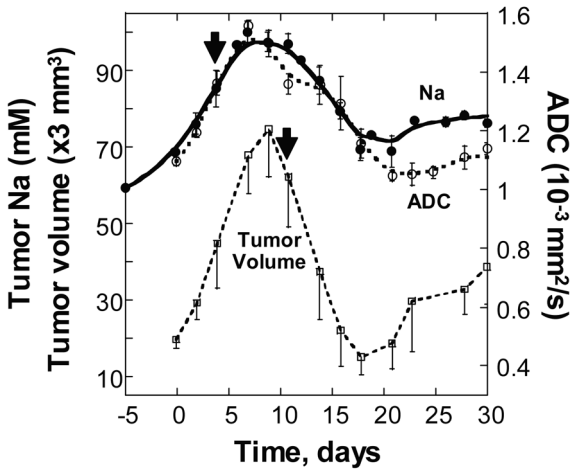

FIG. 8. Comparison of the time dependence of tumor Na concentration (●), ADC of water in the tumor (○), and tumor volume (□) in a BCNU-treated rat glioma model ($n = 5$). Tumor shrinking, statistically observed at day 11, can be predicted a week in advance from an increase in both Na MRI and ADC beginning at day 4 from BCNU chemotherapy.

age, which reveals that Na concentrations can be significantly altered by successful therapeutic intervention.

If we assumed that only a loss of the trans-membrane Na gradient was taking place without membrane destruction, it would have created a different outcome. Sodium and water usually move in the same direction; consequently, the movement of water into intracellular space would lead to cell swelling and to a decrease in ADC values (26–29). Observation in our case of an increase in tumor Na concentration and a simultaneous increase of tumor water ADC during BCNU treatment is most likely due to loss of tumor cell membrane integrity and subsequent changes in tumor due to efficacious treatment.

Many chemotherapeutic agents act by induction of cellular necrosis, which leads to an inability of the cell membrane to maintain its sodium homeostasis. In addition, apoptosis may occur, which is characterized by large cell volume reduction and chromatin condensation (30). Anticancer drug-induced ionic elevations may be closely related with apoptotic changes (31). Sodium overload may have a strong connection with apoptosis and even initiate apoptosis itself, as demonstrated recently (32,33). Thus, the observed intensive sodium uptake following BCNU treatment is reflective of the significant loss of Na homeostasis by corresponding loss of cell membrane integrity due to necrotic and/or apoptotic pathways.

Temporal curves in Fig. 8 indicate that there is a strong correlation between sodium and water diffusion properties in the tumor following therapy. Overlay of the time course of Na tumor MRI signals and ADC values in BCNU-treated 9L glioma (Fig. 8) reveals a very close relationship following BCNU treatment. Correlation of the tumor Na and ADC for the period of BCNU effect is given in Fig. 9. These results present strong evidence for the hypothesis that the ADC rise during positive tumor treatment correlates with Na signal growth and with corresponding tumor cell destruction.

Both Na concentration and changes in ADC values in the treated group were statistically different from untreated group at day 4 after BCNU treatment. Tumor regression was observed on average at day 11 posttreatment. Thus, both Na MRI and ADC were capable of predicting early positive response to anti-cancer therapy ~7 days prior to tumor shrinkage.

Sodium MRI and ADC methods reflect the same cell destruction in the tumor during treatment, yet they detect different properties. Some confirmation of the differences can be seen at the time of tumor regrowth at day 20 and beyond (Fig. 8). ADC returned to pretreatment values as cell membranes regrow and restore additional barriers for water diffusion. At this time, sodium concentrations in the tumor remained higher than pretreatment values, but were similar to the Na content in untreated tumors of the same size (Fig. 5).

The overlay of the time course for Na tumor MRI signals and ADC in untreated 9L rat brain tumors demonstrates more clearly the differences between Na MRI and ADC (Fig. 7). No significant changes in ADC can be seen in the untreated tumor over time, while the Na MRI signal increases progressively. This increase in sodium was steadily observed over time with approximately the same rate for both small and large untreated tumors. Thus, the Na signal increase appears unlikely to be solely the result of a partial volume effect. Similar changes in tumor sodium content were also observed earlier in untreated C6 rat glioma (18). We speculate that most likely two possible yet differing processes can be present simultaneously in untreated tumors. In one process the increase of tumor intracellular Na occurs without cellular destruction. During the other process an increase in Na tissue content occurs as a result of cell destruction due to a partial necrosis (34). Both processes increase Na tumor content but changes of ADC occur in an opposing direction. Thus, a combined effect of two processes can explain the observed Na increase in untreated tumor without changes in ADC,

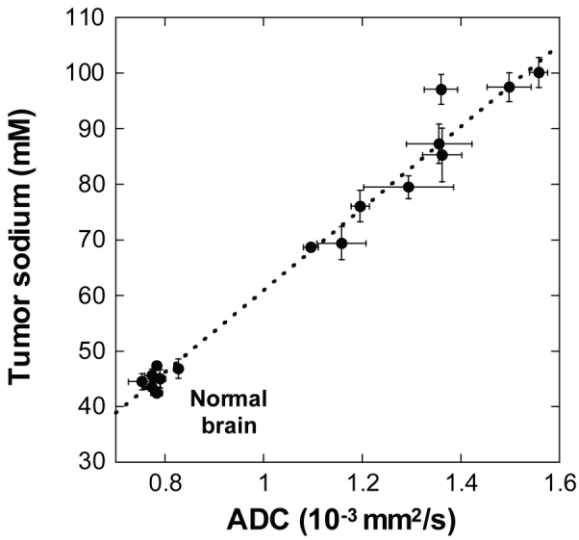

FIG. 9. Correlation of tumor Na and ADC in the 9L rat glioma from data obtained at various time points following a single dose of BCNU ($y = -12.7 + 73.7x$, $R = 0.990$).

as in our experiments the average whole tumor Na concentrations were contrasted to the average ADC values of the tumor.

Tumor cellular changes during BCNU treatment in our 9L rat glioma model was presented in a previous publication (25). From a histologic study during $2 \times LD_{10}$ BCNU treatment, after 9 days cellular density decreased to 25% of the pretreatment value, indicating that approximately 75% of the cells were lost due to chemotherapy destruction. If normal brain has 45 mM Na concentration, the range of possible Na concentrations is 45 to 140 mM. Thus, we can estimate the degree of cell destruction from sodium data. From our Na MRI data it follows that the Na concentration may be increased in the treated tumor up to 2.2 times relative to the normal brain (i.e., 100 mM). Therefore, we can estimate that in a treated tumor ~66% of the brain tumor cells lost Na trans-membrane gradient. This level could be the upper limit of cell destruction as we did not take into consideration that some part of tumor cells can have an increase in intracellular Na without cell destruction. In any case, sodium MRI data correspond reasonably well to the histopathologic decrease in cell density.

The determined values for cell destruction (66–75%) represent tumor cell death at day 7 following the start of BCNU treatment. In our experiments cell kill was determined to be ~1.6, which corresponds to 97% tumor cell destruction (35). However, the parameters "cell destruction" and "cell kill" represent cell changes at different times. Sodium MRI data give information about tumor cell destruction at day 7, while cell kill gives an integrative effect of the BCNU treatment over the course of the entire experimental period.

CONCLUSION

Sodium MRI revealed an increase in Na tumor content following BCNU treatment that correlated with an ADC increase in the 9L rat glioma model. Na tumor content is heterogeneous in all stages of tumor growth in untreated tumors, reflecting the intratumor heterogeneity of gliomas and the presence of spontaneous necrosis. BCNU chemotherapy initiates an intensive tumor Na increase, which reflects a dramatic loss of Na trans-membrane gradient by cell destruction, resulting from a positive response to therapy. Both Na MRI and ADC showed the possibility of early prediction of positive therapy a week in advance in the present experiments.

BCNU, along with many other chemotherapeutic agents and radiation, is capable of initiating cellular necrosis and apoptosis, which are intermediate steps toward tumor mass shrinkage. Unfortunately, few methods can accurately quantify necrosis and apoptosis in vivo. Timely in vivo detection of tumor cell destruction is critically important for evaluating anti-cancer therapies. The intensive sodium uptake during BCNU treatment observed in this study may provide an important tool for detecting the efficacy of therapy and validates the use of proton ADC mapping for assessing tumor cellularity.

ACKNOWLEDGMENTS

The authors thank Daniel Hall and Bradford Moffat for their help with implementation of the experimental protocol and James Sugai for assistance with culture and implantation of the tumor cells.

REFERENCES

1. Jacobs AH, Dittmar C, Winkeler A, Garlip G, Heiss WD. Molecular imaging of gliomas. Mol Imaging 2002;1:309–335.
2. Blasberg RG. Molecular imaging and cancer. Mol Cancer Ther 2003;2: 335–343.
3. Finley RS. Overview of targeted therapies for cancer. Am J Health Syst Pharm 2003;60:S4–S10.
4. Mountz JD, Hsu HC, Wu Q, Liu HG, Zhang HG, Mountz JM. Molecular imaging: new applications for biochemistry. J Cell Biochem Suppl 2002;39:162–171.
5. Gillies RJ, Raghunand N, Karczmar GS, Bhujwalla ZM. MRI of the tumor microenvironment. J Magn Reson Imaging 2002;16:430–450.
6. Boada FE, Shen GX, Chang SY, Thulborn KR. Spectrally weighted twisted projection imaging: reducing T2 signal attenuation effects in fast three-dimensional sodium imaging. Magn Reson Med 1997;38: 1022–1028.
7. Clayton DB, Lenkinski RE. MR imaging of sodium in the human brain with a fast three-dimensional gradient-recalled-echo sequence at 4 T. Acad Radiol 2003;10:358–365.
8. Constantinides CD, Gillen JS, Boada FE, Pomper MG, Bottomley PA. Human skeletal muscle: sodium MR imaging and quantification-potential applications in exercise and disease. Radiology 2000;216:559–568.
9. Borthakur A, Shapiro EM, Akella SV, Gougoutas A, Kneeland JB, Reddy R. Quantifying sodium in the human wrist in vivo by using MR imaging. Radiology 2002;224:598—602.
10. Kaplan O, Kushnir T, Askenazy N, Knubovets T, Navon G. Role of nuclear magnetic resonance spectroscopy (MRS) in cancer diagnosis and treatment: ^{31}P, ^{23}Na, and ^{1}H MRS studies of three models of pancreatic cancer. Cancer Res 1997;57:1452–1459.
11. Seshan V, Germann MJ, Preisig P, Malloy CR, Sherry AD, Bansal N. TmDOTP5- as a ^{23}Na shift reagent for the in vivo rat kidney. Magn Reson Med 1995;34:25–31.
12. Winkler SS. Sodium-23 magnetic resonance brain imaging. Neuroradiology 1990;32:416–420.
13. Perman WH, Turski PA, Houston LW, Glover GH, Hayes CE. Methodology of in vivo human sodium MR imaging at 1.5 T. Radiology 1986; 160:811–820.
14. Ouwerkerk R, Bleich KB, Gillen JS, Pomper MG, Bottomley PA. Tissue sodium concentration in human brain tumors as measured with ^{23}Na MR imaging. Radiology 2003;227:529–537.
15. Kohler S, Preibisch C, Nittka M, Haase A. Fast three-dimensional sodium imaging of human brain. Magma 2001;13:63–69.
16. Ross BD, Moffat BA, Lawrence TS, Mukherji SK, Gebarski SS, Quint DJ, Johnson TD, Junck L, Robertson PL, Muraszko KM, Dong Q, Meyer CR, Bland PH, McConville P, Geng H, Rehemtulla A, Chenevert TL. Evaluation of cancer therapy using diffusion magnetic resonance imaging. Mol Cancer Ther 2003;2:581–587.
17. Chenevert TL, Meyer CR, Moffat BA, Rehemtulla A, Mukherji SK, Gebarski SS, Quint DJ, Robertson PL, Lawrence TS, Junck L, Taylor JM, Johnson TD, Dong Q, Muraszko KM, Brunberg JA, Ross BD. Diffusion MRI: a new strategy for assessment of cancer therapeutic efficacy. Mol Imaging 2002;1:336–343.
18. Thulborn KR, Davis D, Adams H, Gindin T, Zhou J. Quantitative tissue sodium concentration mapping of the growth of focal cerebral tumors with sodium magnetic resonance imaging. Magn Reson Med 1999;41: 351–359.
19. Winter PM, Bansal N. Triple-quantum-filtered (23)Na NMR spectroscopy of subcutaneously implanted 9l gliosarcoma in the rat in the presence of TmDOTP(5–1). J Magn Reson 2001;152:70–78.
20. Winter PM, Poptani H, Bansal N. Effects of chemotherapy by 1,3-bis(2-chloroethyl)-1-nitrosourea on single-quantum- and triple-quantum-filtered ^{23}Na and ^{31}P nuclear magnetic resonance of the subcutaneously implanted 9L glioma. Cancer Res 2001;61:2002–2007.
21. Winter PM, Bansal N. TmDOTP(5-) as a (23)Na shift reagent for the subcutaneously implanted 9L gliosarcoma in rats. Magn Reson Med 2001;45:436–442.
22. Bansal N, Germann MJ, Lazar I, Malloy CR, Sherry AD. In vivo Na-23 MR imaging and spectroscopy of rat brain during TmDOTP5- infusion. J Magn Reson Imaging 1992;2:385–391.
23. Lauterbur PC. Image formation by induced local interactions: examples employing nuclear magnetic resonance. Nature 1973;242:190–191.

24. Christensen JD, Barrere BJ, Boada FE, Vevea JM, Thulborn KR. Quantitative tissue sodium concentration mapping of normal rat brain. Magn Reson Med 1996;36:83–89.
25. Chenevert TL, Stegman LD, Taylor JM, Robertson PL, Greenberg HS, Rehemtulla A, Ross BD. Diffusion magnetic resonance imaging: an early surrogate marker of therapeutic efficacy in brain tumors. J Natl Cancer Inst 2000;92:2029–2036.
26. Lin SP, Song SK, Miller JP, Ackerman JJ, Neil JJ. Direct, longitudinal comparison of (1)H and (23)Na MRI after transient focal cerebral ischemia. Stroke 2001;32:25–932.
27. Thulborn KR, Gindin TS, Davis D, Erb P. Comprehensive MR imaging protocol for stroke management: tissue sodium concentration as a measure of tissue viability in nonhuman primate studies and in clinical studies. Radiology 1999;213:156–166.
28. Wang Y, Hu W, Perez-Trepichio AD, Ng TC, Furlan AJ, Majors AW, Jones SC. Brain tissue sodium is a ticking clock telling time after arterial occlusion in rat focal cerebral ischemia. Stroke 2000;31:1386–1391;discussion 1392.
29. Wang Y, Majors A, Najm I, Xue M, Comair Y, Modic M, Ng TC. Postictal alteration of sodium content and apparent diffusion coefficient in epileptic rat brain induced by kainic acid. Epilepsia 1996;37:1000–1006.
30. Makin G. Targeting apoptosis in cancer chemotherapy. Expert Opin Ther Targets 2002;6:73–84.
31. Kline RP, Wu EX, Petrylak DP, Szabolcs M, Alderson PO, Weisfeldt ML, Cannon P, Katz J. Rapid in vivo monitoring of chemotherapeutic response using weighted sodium magnetic resonance imaging. Clin Cancer Res 2000;6:2146–2156.
32. Bortner CD, Cidlowski JA. Uncoupling cell shrinkage from apoptosis reveals that Na+ influx is required for volume loss during programmed cell death. J Biol Chem 2003;278:39176–39184.
33. Koike T, Tanaka S, Oda T, Ninomiya T. Sodium overload through voltage-dependent Na(+) channels induces necrosis and apoptosis of rat superior cervical ganglion cells in vitro. Brain Res Bull 2000;51:345–355.
34. Joy A, Panicker S, Shapiro JR. Altered nuclear localization of bax protein in BCNU-resistant glioma cells. J Neurooncol 2000;49:117–129.
35. Ross BD, Zhao YJ, Neal ER, Stegman LD, Ercolani M, Ben-Yoseph O, Chenevert TL. Contributions of cell kill and posttreatment tumor growth rates to the repopulation of intracerebral 9L tumors after chemotherapy: an MRI study. Proc Natl Acad Sci USA 1998;95:7012–7017.